

PROTOSTELLAR ACCRETION DISKS RESOLVED WITH THE JCMT-CSO INTERFEROMETER

O. P. LAY,¹ J. E. CARLSTROM,² R. E. HILLS,¹ AND T. G. PHILLIPS²

Received 1994 May 16; accepted 1994 August 4

ABSTRACT

The JCMT-CSO submillimeter interferometer was used to measure the size and orientation of the compact dust continuum emission at 870 μm from the protostellar sources HL Tau and L1551 IRS 5. Assuming an elliptical Gaussian for the brightness distribution and distances of 140 pc, the data are well fitted by semi-major radii to half-maximum brightness and position angles of 60 AU at 126° for HL Tau and 80 AU at 162° for L1551. An upper limit of 50 AU ($0''.4$) is set for the radii along the minor axes, leading to minimum brightness temperatures of 36 K and 28 K, respectively. The elongation in the continuum emission is perpendicular to the outflow axes, as expected for accretion disks. The high brightness indicates substantial column density and mass, further strengthening the accretion disk interpretation. Our observations do not strongly constrain the disk mass; applying an accretion disk model to our data gives a lower limit of $\sim 0.02 M_\odot$ for both sources.

Subject headings: accretion: accretion disks — circumstellar matter — infrared: stars — stars: formation — stars: low-mass, brown dwarfs — stars: pre-main-sequence

1. INTRODUCTION

There can be little doubt that many young stars have circumstellar disks. A survey of pre-main-sequence stars by Beckwith et al. (1990) found evidence for disks in 42% of the objects observed. The original detection of infrared excesses from T Tauri stars (Mendoza 1966) has been followed by detailed modeling of the spectral energy distributions which suggests that the disks have radii of about 100 AU (e.g., Adams, Lada, & Shu 1987; Kenyon & Hartmann 1987), comparable to the size of the early solar nebula.

The thermal continuum flux from a dusty accretion disk is expected to scale with frequency as ν^2 or steeper; the apparent size of a disk will also increase as it becomes increasingly optically thick at higher frequencies within the Rayleigh-Jeans regime. But the residual envelope of infalling dust that surrounds a protostar obscures the core for $\lambda < 0.1$ mm, and it is therefore at submillimeter wavelengths that we stand the best chance of resolving the disks. For the nearest star-forming clouds, 100 AU corresponds to an angular radius of about $0''.7$, so adequate resolution of the disks requires an interferometer with a baseline of at least 150 k λ .

The JCMT-CSO Interferometer comprises the James Clerk Maxwell Telescope and the Caltech Submillimeter Observatory separated by 164 m (189 k λ at $\lambda = 0.87$ mm). Technical aspects of the instrument are described by Carlstrom et al. (1993, 1994). Although the single baseline precludes imaging in the usual sense, the short wavelength and high resolution of the interferometer are ideal for measuring circumstellar disks.

This Letter describes observations made using the interferometer which resolve the circumstellar disks around the protostars L1551 IRS 5 and HL Tau. Both sources are well studied, have bipolar outflows, and were strongly suspected of having disks. Keene & Masson (1990) determined a size ≤ 64 AU for the compact continuum source associated with L1551 IRS 5 using the Owens Valley millimeter interferometer at 2.73

mm. The continuum emission from HL Tau was unresolved in observations at ~ 3 mm (Ohashi et al. 1991; Sargent & Beckwith 1991) and at 1.4 mm (Woody et al. 1989).

2. OBSERVATIONS

The JCMT-CSO interferometer was used to observe L1551 IRS 5 and HL Tau on 1993 November 12 over a period of about 8 hr. The projected length of the baseline varied from 50 k λ to 200 k λ . The quasar 0528+134 was used to monitor the gain of the instrument. We cycled through the three sources about once every hour. The correlator generated spectra of 400 1.25 MHz channels, which were averaged together to produce a 500 MHz bandwidth continuum channel centered at 345.785 GHz. The data were taken with integrations of 10 s and then vector-averaged over 100 s periods. The interferometer is coherent over this relatively short timescale, but the phase response is not yet well determined over longer periods. For this reason only the modulus of the visibility flux was used in the analysis. The average effective single-sideband system temperature was ~ 700 K, equivalent to a noise level of 3 mK or 0.42 Jy in each 100 s data point. The sensitivity of the instrument was 140 Jy K $^{-1}$ ($\pm 20\%$); this relatively low gain was partly due to a problem with the phase switching (now corrected) which does not otherwise affect the results. The 0528+134 data showed no evidence for variation in the system sensitivity during the night. The CO (3–2) transition does lie within the passband, but the spectra show that the contribution to the correlated flux from this line was less than 5%, and care was taken to remove it from the data.

3. MODEL FITTING

Figure 1a shows the visibility flux as a function of projected baseline length for HL Tau. For long baselines the fringe spacing becomes comparable with the source size, and the flux seen by the interferometer is reduced; it is clear that the source has been resolved. A simple Gaussian visibility curve was fitted using a least-squares method. It has a half-width half-maximum corresponding to an angular radius of $0''.4$ or a linear size of 57 AU. The fit is improved by adopting a two-dimensional Gaussian model for the brightness distribution, as

¹ Mullard Radio Astronomy Observatory, Madingley Road, Cambridge CB3 0HE, UK.

² Division of Physics, Mathematics and Astronomy, California Institute of Technology, Pasadena, CA 91125.

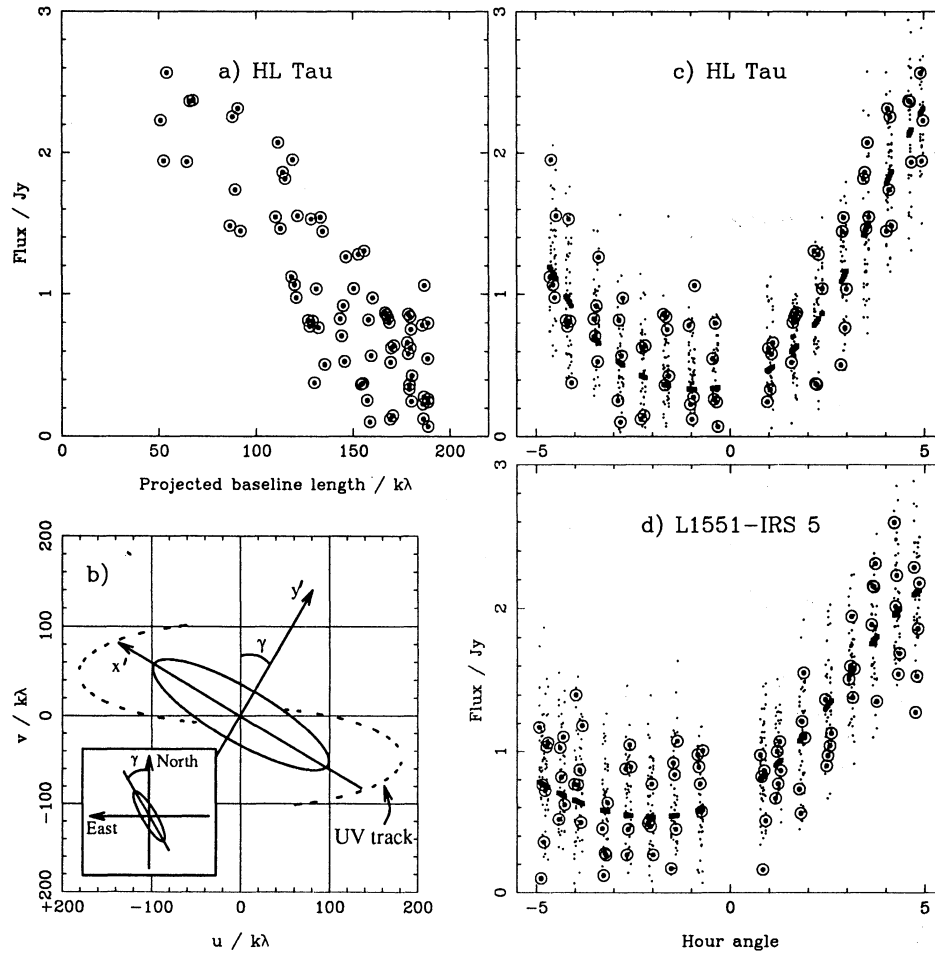


FIG. 1.—(a) The visibility flux of HL Tau at 870 μm detected with the JCMT-CSO interferometer as a function of the projected baseline length, clearly showing that the emission has been resolved. (b) The Gaussian model used to fit the data, shown in the (u, v) plane with the track of the interferometer baseline for the observations of HL Tau. The inset shows the model as it appears on the sky. (c) and (d) Visibility flux as a function of hour angle for HL Tau and L1551 IRS 5, respectively. The actual data are shown by the circled points, and the best-fit model in each case is the series of squares that form a dashed line. The small dots represent the simulated data.

depicted in Figure 1b, and by properly accounting for the amplitude bias introduced to the data by the omission of the phases. There are four parameters to fit: the total flux S_T , the position angle γ , the semimajor radius r_y , and the semiminor radius r_x , both taken to the contour of half-maximum brightness. The visibility flux is then given by

$$\mathcal{V}(u, v) = S_T \exp \left\{ \frac{-\pi^2}{D^2 \ln 2} \times [r_x^2(-u \cos \gamma + v \sin \gamma)^2 + r_y^2(u \sin \gamma + v \cos \gamma)^2] \right\}.$$

Figure 1b shows the model projected on the (u, v) plane with the track of the interferometer baseline as seen by L1551 IRS 5 and HL Tau. For any set of the model parameters, we can calculate the visibility flux predicted for a particular (u, v) and compare it to the actual data. The χ^2 is a maximum likelihood estimator only when the uncertainties have a Gaussian distribution. The modulus of the visibility flux is, however, a positive quantity. In the absence of signal, the noise must be greater than zero and is clearly non-Gaussian; we must use the Rice distribution (Thompson, Moran, & Swenson 1986) to calculate the probability of any data point given a model value. The

shape of a Rice distribution is a function of the signal-to-noise ratio and varies from a Rayleigh distribution when the $\text{SNR} = 0$ to a Gaussian when the $\text{SNR} \gg 1$. Using the Rice distribution as the basis of likelihood, the most probable model was determined by searching the four-dimensional parameter space. Table 1 lists the best-fit parameters for each source. Figures 1c and 1d show the visibility flux as a function of the hour angle of each source. The hour angle uniquely determines the position on the (u, v) track, whereas a given baseline length corresponds to two different orientations (see Fig. 1b). Also shown are the best-fit model curve at a level determined by the system temperature. Note that when the SNR is low there are more points above the model line than below as prescribed by

TABLE 1
DISK PARAMETERS

Source	Disk Flux (Jy)	γ	r_{maj}^a (AU)	r_{min}^a (AU)	T_b (K)	Spectral Index ^b
L1551 IRS 5 ...	$2.24^{+0.28}_{-0.14}$	$162^\circ \pm 18^\circ$	80^{+20}_{-10}	< 52	> 28	2.5
HL Tau	$2.52^{+0.42}_{-0.14}$	$126^\circ \pm 9^\circ$	60^{+10}_{-8}	< 52	> 36	2.7

^a Radius at half-maximum, assuming a distance of 140 pc (Elias 1978).

^b Based on 2.7 mm and 870 μm flux densities.

the Rice distribution. Statistical analysis shows that the scatter in the actual data is consistent with the scatter of the simulated data sets, or in other words, the model is a good fit to the data in each case.

The uncertainties quoted for the fit parameters in Table 1 were derived by a Monte Carlo method; the fitting procedure was applied to each of 50 simulated data sets to give 50 different sets of the parameters. The limits span 90% of the fits to the simulated data sets. No account has been taken of correlations between the four parameters so the ranges are conservative. All the parameters are well constrained for both sources, except the semiminor radii which have upper limits of ~ 50 AU.

4. DISCUSSION

The results listed in Table 1 show that a circularly symmetric brightness distribution is effectively ruled out, and we have detected elongation of both sources. We can compare the orientation of the fitted ellipses with maps of the bipolar outflows for each source (e.g., for HL Tau: Mundt, Ray, & Bührke 1988; Sargent & Beckwith 1991; Hayashi, Ohashi, & Miyama 1993; and for L1551 IRS 5: Snell, Loren, & Plambeck 1980; Bieging, Cohen, & Schwartz 1984; Rodríguez, Cantó, & Torrelles 1986). The fits are consistent with disks lying in the plane perpendicular to the outflows. With only an upper limit on the minor axis radius, it is not possible to derive an angle of inclination or a thickness for the dust distribution.

4.1. Origin of the Submillimeter Continuum Emission

Dusty accretion disks are the most obvious candidate to explain the elongation present in the two sources. However, it is worth checking whether other emission mechanisms and geometries could be wholly responsible for, or partly contribute to, the brightness distribution that we observe. We have considered an infalling envelope, free-free emission, a binary system, and a toroidal distribution of dust.

As Terebey, Chandler, & André (1993) point out, emission from the warm infalling envelope of the parent molecular cloud can be an important source of flux at these wavelengths. Although the interferometer will resolve out the extended emission, the brightness distribution is strongly peaked toward the center and will give some contribution to the detected flux. For HL Tau the interferometer has detected all of the 2.6 Jy measured in a $16''$ beam (Adams, Emerson, & Fuller 1990). Apparently thermal dust emission from the extended, possibly infalling envelope traced by high-resolution CO observations (Sargent & Beckwith 1991; Hayashi et al. 1993) is insignificant compared to the disk emission. For L1551 IRS 5, however, the 2.2 Jy emission associated with the disk accounts for only $\sim 25\%$ of the single-dish flux reported by Keene & Masson (1990).

We modeled the envelope of L1551 IRS 5 as an optically thin sphere of arbitrarily large extent, but with an inner cutoff radius of 50 AU, having $T \propto r^{-0.5}$ and $\rho \propto r^{-1.5}$ (Adams et al. 1987). The flux scale for these models was calibrated using single dish fluxes (Keene & Masson 1990) and the visibility curve for the envelope was then calculated numerically. We estimate that the JCMT-CSO Interferometer will detect a maximum flux of 0.1 Jy from the envelope, just 5% of the flux attributed to the disk. This contribution rises to 0.3 Jy if $T \propto r^{-1.0}$.

Free-free emission from L1551 IRS 5 has been detected with the VLA (Bieging et al. 1984; Rodríguez et al. 1986). Keene & Masson (1990) show that this is unlikely to be an important

source of flux at millimeter and submillimeter wavelengths. The dust and free-free emission components are quite clear for HL Tau (Rodríguez 1994) and by extrapolating the free-free emission to higher frequencies we estimate that it contributes only 1% to the total flux.

The elongated brightness distribution that we attribute to a disk may be due to a binary system with each component possessing a spherically-symmetric dust envelope. Ghez, Neugebauer, & Matthews (1993) used speckle techniques to show that at least 60% of T Tauri stars occurred in multiple systems, but found no evidence for multiplicity in HL Tau. The envelope of L1551 IRS 5 is optically thick at the wavelength they used ($2 \mu\text{m}$) so a multiple system cannot be ruled out in this case. If it is a binary with equal components then our data imply an angular separation of less than $1''$. We also cannot rule out elongation due to a toroidal geometry of dust surrounding a central star.

4.2. Optical Depth and Temperature

The spectral index of the disk emission will reflect the optical depth of the disk and the frequency dependence of the dust emissivity. We can compute the spectral index using our 870 μm flux densities and those determined from interferometric observations at ~ 3 mm (e.g., for HL Tau: Sargent & Beckwith 1991; Ohashi et al. 1991; Hayashi et al. 1993; and for L1551 IRS 5: Keene & Masson 1990; Ohashi et al. 1991). The spectral indices are 2.7 and 2.5 for HL Tau and L1551 IRS 5, respectively.

These low indices suggest that a substantial portion of each disk is optically thick at millimeter and submillimeter wavelengths. A possible alternative is that they are composed of a relatively dilute concentration of grains whose emissivity is weakly dependent on frequency. Pollack et al. (1994) suggest that grains of size 10 μm or more are required to achieve the latter. In both cases much of the disk mass may be hidden: obscured either in the depths of the disk or in the interior of the large grains.

Since we only have an upper limit to angular size along the minor axes we can only set lower limits to the brightness temperature of the disks. These are 36 K for HL Tau and 28 K for L1551 IRS 5. To gain further insight into the disk structure and mass, we must employ a theoretical model for the emission.

4.3. An Accretion Disk Model

We adopt a standard accretion disk model, where temperature and surface density in the disk are power laws in the radius and use the same notation as Beckwith et al. (1990): $T_{\text{disk}} = T_1(r_{\text{disk}}/\text{AU})^{-q}$ and $\Sigma_{\text{disk}} = \Sigma_1(r_{\text{disk}}/\text{AU})^{-p}$. Both actively accreting disks and passive disks illuminated by their star are predicted to have $q = 0.75$ (Lynden-Bell & Pringle 1974; Adams & Shu 1986), but Beckwith et al. (1990) estimate $q \simeq 0.5$ for a number of T Tauri stars. We also assume $1.0 \leq p \leq 1.5$ and take $T_1 = 500$ K. The total flux from the disk is given by $\int_{0.02 \text{ AU}}^{R_d} B_\nu(1 - e^{-\tau}) \cos \theta (2\pi r dr/D^2)$, where B_ν is the Planck function, θ is the inclination of the disk axis to the line of sight, and D is the distance to the source. The optical depth $\tau = \Sigma_{\text{disk}} \kappa_\nu / \cos \theta$, where the specific dust opacity $\kappa_\nu = 0.1(250 \mu\text{m}/\lambda)^\beta \text{ cm}^2 \text{ g}^{-1}$ (Hildebrand 1983). Observed spectral indices and theoretical considerations suggest $0.5 \leq \beta \leq 2.0$.

For each combination of p , q , and β , within the ranges specified above, values of Σ_1 , θ , and the cutoff radius R_d could be found that reproduced the total flux, spectral index, and the

general shape of the visibility curve for each source, using the position angles determined from the Gaussian fitting. A lower limit to the disk mass comes from choosing $p = 1.0$, $q = 0.5$, and $\beta = 0.5$, giving solutions that are optically thick only within ~ 10 AU. For L1551 IRS 5, this mass is $0.02 M_{\odot}$ (e.g., $\Sigma_1 = 170 \text{ g cm}^{-2}$, $\theta = 45^\circ$, $R_d = 200$ AU), and for HL Tau, it is $0.03 M_{\odot}$ (e.g., $\Sigma_1 = 260 \text{ g cm}^{-2}$, $\theta = 45^\circ$, $R_d = 140$ AU). If the dust grains are very large or $T_1 < 500$ K, then the disk masses will be higher than we have estimated here.

Fully optically thick disks also reproduce our data, although the expected spectral index of 2.0 is lower than observed. For $q = 0.75$, examples are $\theta = 53^\circ$, $R_d = 150$ AU for L1551 IRS 5 and $\theta = 38^\circ$, $R_d = 130$ AU for HL Tau. There is no upper limit to the disk mass for this case. The disk mass is therefore not well constrained by our data, but the lower limit of $\sim 0.02 M_{\odot}$ is in line with the minimum mass for the solar nebula and is consistent with previous estimates (e.g., Beckwith et al. (1990).

4.4. Summary

We have made high-resolution submillimeter continuum observations of the young stellar objects HL Tau and L1551

IRS 5, and we find emission that is consistent—in terms of size, orientation, flux, and mass—with the existence of an accretion disk around each source.

L1551 IRS 5 is a much more embedded source than HL Tau and therefore presumably is younger. That the disks are comparable in size and flux may imply that they are well established at a relatively early stage in the protostar's evolution (see also Terebey et al. 1993).

We thank Brian Force, Colin Hall, and Anthony Schinckel for their major technical contributions; Chris Mayer, Mary Fuka, and Ken Young for invaluable work on software; and many others of the JCMT and CSO staff. We also thank the referee for a number of useful suggestions. O. P. L. acknowledges the receipt of a PPARC studentship and J. E. C. an NSF-YI award. The JCMT is operated by the Royal Observatories on behalf of the Particle Physics and Astronomy Research Council of the United Kingdom, the Netherlands Organization for Scientific Research, and the National Research Council of Canada. Research at the CSO is supported by NSF grant 90-15755.

REFERENCES

- Adams, F. C., Emerson, J. P., & Fuller, G. A. 1990, *ApJ*, 357, 606
 Adams, F. C., Lada, C. J., & Shu, F. H. 1987, *ApJ*, 312, 788
 Adams, F. C., & Shu, F. H. 1986, *ApJ*, 308, 836
 Beckwith, S. V. W., Sargent, A. I., Chini, R. S., & Güsten, R. 1990, *AJ*, 99, 924
 Bieging, J. H., Cohen, M., & Schwartz, P. R. 1984, *ApJ*, 282, 699
 Carlstrom, J. E., Hills, R. E., Lay, O. P., Force, B. F., Hall, C. G., Phillips, T. G., & Schinckel, A. E. 1993, in *IAU Colloq. 140, Astronomy with Millimeter and Submillimeter Wave Interferometry*, ed. M. Ishiguro & Wm. J. Welch (ASP Conf. Proc., 59), 35
 Carlstrom, J. E., Lay, O. P., Hills, R. E., Phillips, T. G., Force, B., Hall, C. G., Mayer, C., & Schinckel, A. E. 1994, in preparation
 Elias, J. 1978, *ApJ*, 224, 857
 Ghez, A. M., Neugebauer, G., & Matthews, K. 1993, *AJ*, 106, 2005
 Hayashi, M., Ohashi, N., & Miyama, S. 1993, *ApJ*, 418, L71
 Hildebrand, R. H. 1983, *QJRAS*, 24, 267
 Keene, J., & Masson, C. R. 1990, *ApJ*, 355, 635
 Kenyon, S. J., & Hartmann, L. 1987, *ApJ*, 323, 714
 Lynden-Bell, D., & Pringle, J. E. 1974, *MNRAS*, 168, 603
 Mendoza, E. E. 1966, *ApJ*, 143, 1010
 Mundt, R., Ray, T. P., & Bührke, T. 1988, *ApJ*, 333, L69
 Ohashi, N., Kawabe, R., Hayashi, M., & Ishiguro, M. 1991, *AJ*, 102, 2054
 Pollack, J. B., Hollenbach, D., Beckwith, S., Simonelli, D. P., Roush, T., & Fong, W. 1994, *ApJ*, 421, 615
 Rodriguez, L. F. 1994, *Rev. Mexicana Astron. Af.*, in press
 Rodriguez, L. F., Cantó, J., & Torrelles, J. M. 1986, *ApJ*, 301, L25
 Sargent, A. I., & Beckwith, S. V. W. 1991, *ApJ*, 382, L31
 Snell, R. L., Loren, R. B., & Plambeck, R. L. 1980, *ApJ*, 239, L17
 Terebey, S., Chandler, C. J., & André, P. 1993, *ApJ*, 414, 759
 Thompson, A. R., Moran, J. M., & Swenson, G. W. 1986, *Interferometry and Synthesis in Radio Astronomy* (New York: Wiley-Interscience)
 Woody, D. P., Scott, S. L., Scoville, N. Z., Mundy, L. G., Sargent, A. I., Padin, S., Tinney, C. G., & Wilson, C. D. 1990, *ApJ*, 337, L41
 Yamashita, T., Hodapp, K.-W., & Moore, T. J. P. 1994, *ApJ*, 422, L21